Search for di-muon decays of a low-mass Higgs boson in radiative decays of the Υ(1S)

J. P. Lees *et al.* (BABAR Collaboration)

Phys. Rev. D **87**, 031102 — Published 15 February 2013

DOI: 10.1103/PhysRevD.87.031102

BaBar-PUB-12/023
SLAC-PUB-15252

Search for di-muon decays of a low-mass Higgs boson in radiative decays of the $\Upsilon(1S)$

J. P. Lees,[1] V. Poireau,[1] V. Tisserand,[1] J. Garra Tico,[2] E. Grauges,[2] A. Palano[ab],[3] G. Eigen,[4] B. Stugu,[4] D. N. Brown,[5] L. T. Kerth,[5] Yu. G. Kolomensky,[5] G. Lynch,[5] H. Koch,[6] T. Schroeder,[6] D. J. Asgeirsson,[7] C. Hearty,[7] T. S. Mattison,[7] J. A. McKenna,[7] R. Y. So,[7] A. Khan,[8] V. E. Blinov,[9] A. R. Buzykaev,[9] V. P. Druzhinin,[9] V. B. Golubev,[9] E. A. Kravchenko,[9] A. P. Onuchin,[9] S. I. Serednyakov,[9] Yu. I. Skovpen,[9] E. P. Solodov,[9] K. Yu. Todyshev,[9] A. N. Yushkov,[9] M. Bondioli,[10] D. Kirkby,[10] A. J. Lankford,[10] M. Mandelkern,[10] H. Atmacan,[11] J. W. Gary,[11] F. Liu,[11] O. Long,[11] G. M. Vitug,[11] C. Campagnari,[12] T. M. Hong,[12] D. Kovalskyi,[12] J. D. Richman,[12] C. A. West,[12] A. M. Eisner,[13] J. Kroseberg,[13] W. S. Lockman,[13] A. J. Martinez,[13] B. A. Schumm,[13] A. Seiden,[13] D. S. Chao,[14] C. H. Cheng,[14] B. Echenard,[14] K. T. Flood,[14] D. G. Hitlin,[14] P. Ongmongkolkul,[14] F. C. Porter,[14] A. Y. Rakitin,[14] R. Andreassen,[15] Z. Huard,[15] B. T. Meadows,[15] M. D. Sokoloff,[15] L. Sun,[15] P. C. Bloom,[16] W. T. Ford,[16] A. Gaz,[16] U. Nauenberg,[16] J. G. Smith,[16] S. R. Wagner,[16] R. Ayad,[17, *] W. H. Toki,[17] B. Spaan,[18] K. R. Schubert,[19] R. Schwierz,[19] D. Bernard,[20] M. Verderi,[20] P. J. Clark,[21] S. Playfer,[21] D. Bettoni[a],[22] C. Bozzi[a],[22] R. Calabrese[ab],[22] G. Cibinetto[ab],[22] E. Fioravanti[ab],[22] I. Garzia[ab],[22] E. Luppi[ab],[22] L. Piemontese[a],[22] V. Santoro[a],[22] R. Baldini-Ferroli,[23] A. Calcaterra,[23] R. de Sangro,[23] G. Finocchiaro,[23] P. Patteri,[23] I. M. Peruzzi,[23, †] M. Piccolo,[23] M. Rama,[23] A. Zallo,[23] R. Contri[ab],[24] E. Guido[ab],[24] M. Lo Vetere[ab],[24] M. R. Monge[ab],[24] S. Passaggio[a],[24] C. Patrignani[ab],[24] E. Robutti[a],[24] B. Bhuyan,[25] V. Prasad,[25] C. L. Lee,[26] M. Morii,[26] A. J. Edwards,[27] A. Adametz,[28] U. Uwer,[28] H. M. Lacker,[29] T. Lueck,[29] P. D. Dauncey,[30] U. Mallik,[31] C. Chen,[32] J. Cochran,[32] W. T. Meyer,[32] S. Prell,[32] A. E. Rubin,[32] A. V. Gritsan,[33] Z. J. Guo,[33] N. Arnaud,[34] M. Davier,[34] D. Derkach,[34] G. Grosdidier,[34] F. Le Diberder,[34] A. M. Lutz,[34] B. Malaescu,[34] P. Roudeau,[34] M. H. Schune,[34] A. Stocchi,[34] G. Wormser,[34] D. J. Lange,[35] D. M. Wright,[35] C. A. Chavez,[36] J. P. Coleman,[36] J. R. Fry,[36] E. Gabathuler,[36] D. E. Hutchcroft,[36] D. J. Payne,[36] C. Touramanis,[36] A. J. Bevan,[37] F. Di Lodovico,[37] R. Sacco,[37] M. Sigamani,[37] G. Cowan,[38] D. N. Brown,[39] C. L. Davis,[39] A. G. Denig,[40] M. Fritsch,[40] W. Gradl,[40] K. Griessinger,[40] A. Hafner,[40] E. Prencipe,[40] R. J. Barlow,[41, ‡] G. Jackson,[41] G. D. Lafferty,[41] E. Behn,[42] R. Cenci,[42] B. Hamilton,[42] A. Jawahery,[42] D. A. Roberts,[42] C. Dallapiccola,[43] R. Cowan,[44] D. Dujmic,[44] G. Sciolla,[44] R. Cheaib,[45] D. Lindemann,[45] P. M. Patel,[45, §] S. H. Robertson,[45] P. Biassoni[ab],[46] N. Neri[a],[46] F. Palombo[ab],[46] S. Stracka[ab],[46] L. Cremaldi,[47] R. Godang,[47, ¶] R. Kroeger,[47] P. Sonnek,[47] D. J. Summers,[47] X. Nguyen,[48] M. Simard,[48] P. Taras,[48] G. De Nardo[ab],[49] D. Monorchio[ab],[49] G. Onorato[ab],[49] C. Sciacca[ab],[49] M. Martinelli,[50] G. Raven,[50] C. P. Jessop,[51] J. M. LoSecco,[51] W. F. Wang,[51] K. Honscheid,[52] R. Kass,[52] J. Brau,[53] R. Frey,[53] N. B. Sinev,[53] D. Strom,[53] E. Torrence,[53] E. Feltresi[ab],[54] N. Gagliardi[ab],[54] M. Margoni[ab],[54] M. Morandin[a],[54] M. Posocco[a],[54] M. Rotondo[a],[54] G. Simi[a],[54] F. Simonetto[ab],[54] R. Stroili[ab],[54] S. Akar,[55] E. Ben-Haim,[55] M. Bomben,[55] G. R. Bonneaud,[55] H. Briand,[55] G. Calderini,[55] J. Chauveau,[55] O. Hamon,[55] Ph. Leruste,[55] G. Marchiori,[55] J. Ocariz,[55] S. Sitt,[55] M. Biasini[ab],[56] E. Manoni[ab],[56] S. Pacetti[ab],[56] A. Rossi[ab],[56] C. Angelini[ab],[57] G. Batignani[ab],[57] S. Bettarini[ab],[57] M. Carpinelli[ab],[57, **] G. Casarosa[ab],[57] A. Cervelli[ab],[57] F. Forti[ab],[57] M. A. Giorgi[ab],[57] A. Lusiani[ac],[57] B. Oberhof[ab],[57] E. Paoloni[ab],[57] A. Perez[a],[57] G. Rizzo[ab],[57] J. J. Walsh[a],[57] D. Lopes Pegna,[58] J. Olsen,[58] A. J. S. Smith,[58] F. Anulli[a],[59] R. Faccini[ab],[59] F. Ferrarotto[a],[59] F. Ferroni[ab],[59] M. Gaspero[ab],[59] L. Li Gioi[a],[59] M. A. Mazzoni[a],[59] G. Piredda[a],[59] C. Bünger,[60] O. Grünberg,[60] T. Hartmann,[60] T. Leddig,[60] C. Voß,[60] R. Waldi,[60] T. Adye,[61] E. O. Olaiya,[61] F. F. Wilson,[61] S. Emery,[62] G. Hamel de Monchenault,[62] G. Vasseur,[62] Ch. Yèche,[62] D. Aston,[63] D. J. Bard,[63] R. Bartoldus,[63] J. F. Benitez,[63] C. Cartaro,[63] M. R. Convery,[63] J. Dorfan,[63] G. P. Dubois-Felsmann,[63] W. Dunwoodie,[63] M. Ebert,[63] R. C. Field,[63] M. Franco Sevilla,[63] B. G. Fulsom,[63] A. M. Gabareen,[63] M. T. Graham,[63] P. Grenier,[63] C. Hast,[63] W. R. Innes,[63] M. H. Kelsey,[63] P. Kim,[63] M. L. Kocian,[63] D. W. G. S. Leith,[63] P. Lewis,[63] B. Lindquist,[63] S. Luitz,[63] V. Luth,[63] H. L. Lynch,[63] D. B. MacFarlane,[63] D. R. Muller,[63] H. Neal,[63] S. Nelson,[63] M. Perl,[63] T. Pulliam,[63] B. N. Ratcliff,[63] A. Roodman,[63] A. A. Salnikov,[63] R. H. Schindler,[63] A. Snyder,[63] D. Su,[63] M. K. Sullivan,[63] J. Va'vra,[63] A. P. Wagner,[63] W. J. Wisniewski,[63] M. Wittgen,[63] D. H. Wright,[63] H. W. Wulsin,[63] C. C. Young,[63] V. Ziegler,[63] W. Park,[64] M. V. Purohit,[64] R. M. White,[64] J. R. Wilson,[64] A. Randle-Conde,[65] S. J. Sekula,[65] M. Bellis,[66] P. R. Burchat,[66] T. S. Miyashita,[66] E. M. T. Puccio,[66] M. S. Alam,[67] J. A. Ernst,[67] R. Gorodeisky,[68] N. Guttman,[68] D. R. Peimer,[68] A. Soffer,[68] S. M. Spanier,[69] J. L. Ritchie,[70] A. M. Ruland,[70] R. F. Schwitters,[70] B. C. Wray,[70] J. M. Izen,[71] X. C. Lou,[71] F. Bianchi[ab],[72] D. Gamba[ab],[72] S. Zambito[ab],[72] L. Lanceri[ab],[73] L. Vitale[ab],[73] F. Martinez-Vidal,[74] A. Oyanguren,[74]

P. Villanueva-Perez,[74] H. Ahmed,[75] J. Albert,[75] Sw. Banerjee,[75] F. U. Bernlochner,[75] H. H. F. Choi,[75] G. J. King,[75] R. Kowalewski,[75] M. J. Lewczuk,[75] I. M. Nugent,[75] J. M. Roney,[75] R. J. Sobie,[75] N. Tasneem,[75] T. J. Gershon,[76] P. F. Harrison,[76] T. E. Latham,[76] H. R. Band,[77] S. Dasu,[77] Y. Pan,[77] R. Prepost,[77] and S. L. Wu[77]

(The *BABAR* Collaboration)

[1]*Laboratoire d'Annecy-le-Vieux de Physique des Particules (LAPP), Université de Savoie, CNRS/IN2P3, F-74941 Annecy-Le-Vieux, France*

[2]*Universitat de Barcelona, Facultat de Fisica, Departament ECM, E-08028 Barcelona, Spain*

[3]*INFN Sezione di Bari[a]; Dipartimento di Fisica, Università di Bari[b], I-70126 Bari, Italy*

[4]*University of Bergen, Institute of Physics, N-5007 Bergen, Norway*

[5]*Lawrence Berkeley National Laboratory and University of California, Berkeley, California 94720, USA*

[6]*Ruhr Universität Bochum, Institut für Experimentalphysik 1, D-44780 Bochum, Germany*

[7]*University of British Columbia, Vancouver, British Columbia, Canada V6T 1Z1*

[8]*Brunel University, Uxbridge, Middlesex UB8 3PH, United Kingdom*

[9]*Budker Institute of Nuclear Physics, Novosibirsk 630090, Russia*

[10]*University of California at Irvine, Irvine, California 92697, USA*

[11]*University of California at Riverside, Riverside, California 92521, USA*

[12]*University of California at Santa Barbara, Santa Barbara, California 93106, USA*

[13]*University of California at Santa Cruz, Institute for Particle Physics, Santa Cruz, California 95064, USA*

[14]*California Institute of Technology, Pasadena, California 91125, USA*

[15]*University of Cincinnati, Cincinnati, Ohio 45221, USA*

[16]*University of Colorado, Boulder, Colorado 80309, USA*

[17]*Colorado State University, Fort Collins, Colorado 80523, USA*

[18]*Technische Universität Dortmund, Fakultät Physik, D-44221 Dortmund, Germany*

[19]*Technische Universität Dresden, Institut für Kern- und Teilchenphysik, D-01062 Dresden, Germany*

[20]*Laboratoire Leprince-Ringuet, Ecole Polytechnique, CNRS/IN2P3, F-91128 Palaiseau, France*

[21]*University of Edinburgh, Edinburgh EH9 3JZ, United Kingdom*

[22]*INFN Sezione di Ferrara[a]; Dipartimento di Fisica, Università di Ferrara[b], I-44100 Ferrara, Italy*

[23]*INFN Laboratori Nazionali di Frascati, I-00044 Frascati, Italy*

[24]*INFN Sezione di Genova[a]; Dipartimento di Fisica, Università di Genova[b], I-16146 Genova, Italy*

[25]*Indian Institute of Technology Guwahati, Guwahati, Assam, 781 039, India*

[26]*Harvard University, Cambridge, Massachusetts 02138, USA*

[27]*Harvey Mudd College, Claremont, California 91711, USA*

[28]*Universität Heidelberg, Physikalisches Institut, Philosophenweg 12, D-69120 Heidelberg, Germany*

[29]*Humboldt-Universität zu Berlin, Institut für Physik, Newtonstr. 15, D-12489 Berlin, Germany*

[30]*Imperial College London, London, SW7 2AZ, United Kingdom*

[31]*University of Iowa, Iowa City, Iowa 52242, USA*

[32]*Iowa State University, Ames, Iowa 50011-3160, USA*

[33]*Johns Hopkins University, Baltimore, Maryland 21218, USA*

[34]*Laboratoire de l'Accélérateur Linéaire, IN2P3/CNRS et Université Paris-Sud 11, Centre Scientifique d'Orsay, B. P. 34, F-91898 Orsay Cedex, France*

[35]*Lawrence Livermore National Laboratory, Livermore, California 94550, USA*

[36]*University of Liverpool, Liverpool L69 7ZE, United Kingdom*

[37]*Queen Mary, University of London, London, E1 4NS, United Kingdom*

[38]*University of London, Royal Holloway and Bedford New College, Egham, Surrey TW20 0EX, United Kingdom*

[39]*University of Louisville, Louisville, Kentucky 40292, USA*

[40]*Johannes Gutenberg-Universität Mainz, Institut für Kernphysik, D-55099 Mainz, Germany*

[41]*University of Manchester, Manchester M13 9PL, United Kingdom*

[42]*University of Maryland, College Park, Maryland 20742, USA*

[43]*University of Massachusetts, Amherst, Massachusetts 01003, USA*

[44]*Massachusetts Institute of Technology, Laboratory for Nuclear Science, Cambridge, Massachusetts 02139, USA*

[45]*McGill University, Montréal, Québec, Canada H3A 2T8*

[46]*INFN Sezione di Milano[a]; Dipartimento di Fisica, Università di Milano[b], I-20133 Milano, Italy*

[47]*University of Mississippi, University, Mississippi 38677, USA*

[48]*Université de Montréal, Physique des Particules, Montréal, Québec, Canada H3C 3J7*

[49]*INFN Sezione di Napoli[a]; Dipartimento di Scienze Fisiche, Università di Napoli Federico II[b], I-80126 Napoli, Italy*

[50]*NIKHEF, National Institute for Nuclear Physics and High Energy Physics, NL-1009 DB Amsterdam, The Netherlands*

[51]*University of Notre Dame, Notre Dame, Indiana 46556, USA*

[52]*Ohio State University, Columbus, Ohio 43210, USA*

[53]*University of Oregon, Eugene, Oregon 97403, USA*

[54]*INFN Sezione di Padova[a]; Dipartimento di Fisica, Università di Padova[b], I-35131 Padova, Italy*

[55]Laboratoire de Physique Nucléaire et de Hautes Energies, IN2P3/CNRS, Université Pierre et Marie Curie-Paris6, Université Denis Diderot-Paris7, F-75252 Paris, France
[56]INFN Sezione di Perugia[a]; Dipartimento di Fisica, Università di Perugia[b], I-06100 Perugia, Italy
[57]INFN Sezione di Pisa[a]; Dipartimento di Fisica, Università di Pisa[b]; Scuola Normale Superiore di Pisa[c], I-56127 Pisa, Italy
[58]Princeton University, Princeton, New Jersey 08544, USA
[59]INFN Sezione di Roma[a]; Dipartimento di Fisica, Università di Roma La Sapienza[b], I-00185 Roma, Italy
[60]Universität Rostock, D-18051 Rostock, Germany
[61]Rutherford Appleton Laboratory, Chilton, Didcot, Oxon, OX11 0QX, United Kingdom
[62]CEA, Irfu, SPP, Centre de Saclay, F-91191 Gif-sur-Yvette, France
[63]SLAC National Accelerator Laboratory, Stanford, California 94309 USA
[64]University of South Carolina, Columbia, South Carolina 29208, USA
[65]Southern Methodist University, Dallas, Texas 75275, USA
[66]Stanford University, Stanford, California 94305-4060, USA
[67]State University of New York, Albany, New York 12222, USA
[68]Tel Aviv University, School of Physics and Astronomy, Tel Aviv, 69978, Israel
[69]University of Tennessee, Knoxville, Tennessee 37996, USA
[70]University of Texas at Austin, Austin, Texas 78712, USA
[71]University of Texas at Dallas, Richardson, Texas 75083, USA
[72]INFN Sezione di Torino[a]; Dipartimento di Fisica Sperimentale, Università di Torino[b], I-10125 Torino, Italy
[73]INFN Sezione di Trieste[a]; Dipartimento di Fisica, Università di Trieste[b], I-34127 Trieste, Italy
[74]IFIC, Universitat de Valencia-CSIC, E-46071 Valencia, Spain
[75]University of Victoria, Victoria, British Columbia, Canada V8W 3P6
[76]Department of Physics, University of Warwick, Coventry CV4 7AL, United Kingdom
[77]University of Wisconsin, Madison, Wisconsin 53706, USA

We search for di-muon decays of a low-mass Higgs boson (A^0) produced in radiative $\Upsilon(1S)$ decays. The $\Upsilon(1S)$ sample is selected by tagging the pion pair in the $\Upsilon(2S,3S) \to \pi^+\pi^-\Upsilon(1S)$ transitions, using a data sample of 92.8×10^6 $\Upsilon(2S)$ and 116.8×10^6 $\Upsilon(3S)$ events collected by the *BABAR* detector. We find no evidence for A^0 production and set 90% confidence level upper limits on the product branching fraction $\mathcal{B}(\Upsilon(1S) \to \gamma A^0) \times \mathcal{B}(A^0 \to \mu^+\mu^-)$ in the range of $(0.28 - 9.7) \times 10^{-6}$ for $0.212 \leq m_{A^0} \leq 9.20$ GeV/c^2. The results are combined with our previous measurements of $\Upsilon(2S,3S) \to \gamma A^0$, $A^0 \to \mu^+\mu^-$ to set limits on the effective coupling of the b-quark to the A^0.

PACS numbers: 12.60.Fr, 12.60.Jv, 13.20.Gd, 13.35.Bv, 14.40.Ndq, 14.40.Pq, 14.80.Da

Many extensions of the Standard Model (SM), such as the Next-to-Minimal Supersymmetric Standard Model (NMSSM), include a light Higgs boson [1, 2]. The Minimal Supersymmetric Standard Model (MSSM) [3] solves the hierarchy problem of the SM, whose superpotential contains a supersymmetric Higgs mass parameter, μ, that contributes to the masses of the Higgs bosons. The MSSM fails to explain why the value of the μ-parameter is of the order of the electroweak scale, which is many orders of magnitude below the next natural scale, the Planck scale. The NMSSM solves this so-called "μ-problem" [4] by adding a singlet chiral superfield to the MSSM, generating an effective μ-term. As a result, the NMSSM Higgs sector contains a total of three neutral *CP*-even, two neutral *CP*-odd, and two charged Higgs bosons. The lightest *CP*-odd Higgs boson (A^0) could have a mass smaller than twice the mass of the b-quark [1], making it detectable via radiative $\Upsilon(nS) \to \gamma A^0$ ($n = 1, 2, 3$) decays [5].

The coupling of the A^0 field to up-type (down-type) fermion pairs is proportional to $\cos\theta_{\rm A}\cot\beta$ ($\cos\theta_{\rm A}\tan\beta$), where $\theta_{\rm A}$ is the mixing angle between the singlet component and the MSSM component of the A^0, and $\tan\beta$ is the ratio of the vacuum expectation values of the up and down type Higgs doublets. The branching fraction of $\Upsilon(1S) \to \gamma A^0$ could be as large as 10^{-4} depending on the values of the A^0 mass, $\tan\beta$ and $\cos\theta_{\rm A}$ [2]. Constraints on the low-mass NMSSM Higgs sector are also important for interpreting the SM Higgs sector [6].

BABAR has previously searched for A^0 production in several final states [7–10], including $\Upsilon(2S,3S) \to \gamma A^0, A^0 \to \mu^+\mu^-$ [7]. Similar searches have been performed by CLEO in the di-muon and di-tau final states in radiative $\Upsilon(1S)$ decays [11], and more recently by BESIII in $J/\psi \to \gamma A^0, A^0 \to \mu^+\mu^-$ [12], and by the CMS

*Now at the University of Tabuk, Tabuk 71491, Saudi Arabia
†Also with Università di Perugia, Dipartimento di Fisica, Perugia, Italy
‡Now at the University of Huddersfield, Huddersfield HD1 3DH, UK
§Deceased
¶Now at University of South Alabama, Mobile, Alabama 36688, USA
**Also with Università di Sassari, Sassari, Italy

experiment in $pp \to A^0$, $A^0 \to \mu^+\mu^-$ [13]. These results have ruled out a substantial fraction of the NMSSM parameter space [14].

We report herein a search for a di-muon resonance in the fully reconstructed decay chain of $\Upsilon(2S,3S) \to \pi^+\pi^-\Upsilon(1S)$, $\Upsilon(1S) \to \gamma A^0$, $A^0 \to \mu^+\mu^-$. This search is based on a sample of $(92.8 \pm 0.8) \times 10^6$ $\Upsilon(2S)$ and $(116.8 \pm 1.0) \times 10^6$ $\Upsilon(3S)$ mesons collected by the *BABAR* detector at the PEP-II asymmetric-energy e^+e^- collider located at the SLAC National Accelerator Laboratory. A sample of $\Upsilon(1S)$ mesons is selected by tagging the di-pion transition, which results in a substantial background reduction compared to direct searches of A^0 in $\Upsilon(2S,3S) \to \gamma A^0$ decays. We assume that the light Higgs boson that we search for is a scalar or pseudoscalar particle with a negligible decay width compared to the experimental resolution [15].

The *BABAR* detector is described in detail elsewhere [16, 17]. Charged particle momenta are measured in a five-layer double-sided silicon vertex tracker and a 40-layer drift chamber, both operating in a 1.5 T solenoidal magnetic field. Charged particle identification (PID) is performed using a ring-imaging Cherenkov detector and the energy loss ($\mathrm{d}E/\mathrm{d}x$) in the tracking system. Photon and electron energies are measured in a CsI(Tl) electromagnetic calorimeter, while muons are identified in the instrumented magnetic flux return of the magnet.

Monte Carlo (MC) simulated events are used to study the detector acceptance and to optimize the event selection procedure. The EvtGen package [18] is used to simulate the $e^+e^- \to q\overline{q}$ $(q = u, d, s, c)$ and generic $\Upsilon(2S,3S)$ production, BHWIDE [19] to simulate the Bhabha scattering, and KK2F [20] to simulate the processes $e^+e^- \to (\gamma)\mu^+\mu^-$ and $e^+e^- \to (\gamma)\tau^+\tau^-$. Dedicated MC samples of $\Upsilon(2S,3S)$ generic decays to $\pi^+\pi^-\Upsilon(1S)$ with $\Upsilon(1S) \to \gamma\mu^+\mu^-$ decays, hereafter refered to as the "non-resonant di-muon decays" are also generated. Signal events are generated using a phase-space (P-wave) model for the $A^0 \to \mu^+\mu^-$ ($\Upsilon(1S) \to \gamma A^0$) decay, and the hadronic matrix elements measured by the CLEO experiment [21] are used for the $\Upsilon(2S,3S) \to \pi^+\pi^-\Upsilon(1S)$ modeling. The detector response is simulated by GEANT4 [22] and the time-dependent detector effects, such as the variation of the detector performance over the data-taking period and the beam related backgrounds, are included in the simulation. A sample corresponding to about 5% of the dataset is used to validate the selection and fitting procedure. To avoid bias, this sample is discarded from the final dataset. We perform a blind analysis, where the rest of the $\Upsilon(2S,3S)$ datasets are blinded until the analysis procedure is frozen.

We select events containing exactly four charged tracks and a single energetic photon with a center-of-mass (CM) energy larger than 200 MeV. The tracks are required to have a distance of closest approach to the interaction point of less than 1.5 cm in the plane transverse to the beam axis and less than 2.5 cm along the beam axis. At least one of the tracks must be identified as a muon by particle ID algorithms; the probability for misidentifying a charged pion as a muon is 3%. Additional photons with CM energies below the threshold of 200 MeV are also allowed to be present in the events. The two highest momentum tracks in the CM frame with opposite charge are assumed to be muon candidates and are required to originate from a common vertex to form the A^0 candidates.

The $\Upsilon(1S)$ candidate is reconstructed by combining the A^0 candidate with the energetic photon candidate and by requiring the invariant mass to be between 9.0 and 9.8 GeV/c^2. The $\Upsilon(2S,3S)$ candidates are formed by combining the $\Upsilon(1S)$ candidate with the two remaining tracks, assumed to be pions. The di-pion invariant mass must be in the range $[2m_\pi, (m_{\Upsilon(2S,3S)} - m_{\Upsilon(1S)})]$, compatible with the kinematic boundaries of the $\Upsilon(2S,3S) \to \pi^+\pi^-\Upsilon(1S)$ decay. The entire decay chain is then fit by imposing the decay vertex of the $\Upsilon(2S,3S)$ candidate to be constrained to the beam interaction region, and a mass constraint on the $\Upsilon(1S)$ and $\Upsilon(2S,3S)$ candidates, as well as requiring the energy of the $\Upsilon(2S,3S)$ candidate to be consistent with the e^+e^- CM energy. These constraints improve the resolution of the di-muon invariant mass to be less than 10 MeV/c^2.

To improve the purity of the $\Upsilon(1S)$ sample, we train a Random Forest (RF) classifier [23] on simulated signal and background events, using variables that distinguish signal from background in the $\Upsilon(2S,3S) \to \pi^+\pi^-\Upsilon(1S)$ transitions. The following quantities are used as inputs to the classifier: the cosine of the angle between the two pion candidates in the laboratory frame, the transverse momentum of the di-pion system in the laboratory frame, the azimuthal angle and transverse momentum of each pion, the di-pion invariant mass ($m_{\pi\pi}$), the pion helicity angle, the transverse position of the di-pion vertex and the mass recoiling against the di-pion system, defined as $m_{\rm recoil} = \sqrt{s + m_{\pi\pi}^2 - 2\sqrt{s}E_{\pi\pi}^{CM}}$, where $\sqrt{s}$ is the e^+e^- CM energy and $E_{\pi\pi}^{CM}$ is the CM energy of the di-pion system. For signal-like events, the $m_{\rm recoil}$ distribution peaks at the mass of the $\Upsilon(1S)$, with a mass resolution of about 3 MeV/c^2. The RF output peaks at 1 for signal-like candidates and peaks at 0 for the background-like candidates. The optimum value of the RF selection is chosen to maximize Punzi's figure-of-merit, $\epsilon/(0.5N_\sigma + \sqrt{B})$ [24], where $N_\sigma = 3$ is the number of standard deviations desired from the result, and ϵ and B are the average efficiency and background yield over a broad m_{A^0} range ($0.212 - 9.20$ GeV/c^2), respectively.

A total of 11,136 $\Upsilon(2S)$ and 3,857 $\Upsilon(3S)$ candidates are selected by these criteria. Figures 1 and 2 show the distributions of the $m_{\rm recoil}$ and di-muon reduced mass, $m_{\rm red} = \sqrt{m_{\mu^+\mu^-}^2 - 4m_\mu^2}$, together with the background prediction estimated from the MC samples, which are dominated by the non-resonant di-muon decays. The reduced mass is equal to twice the momentum of the di-muon system in the rest frame of the A^0, and has a smooth distribution in the region of the kinematic thresh-

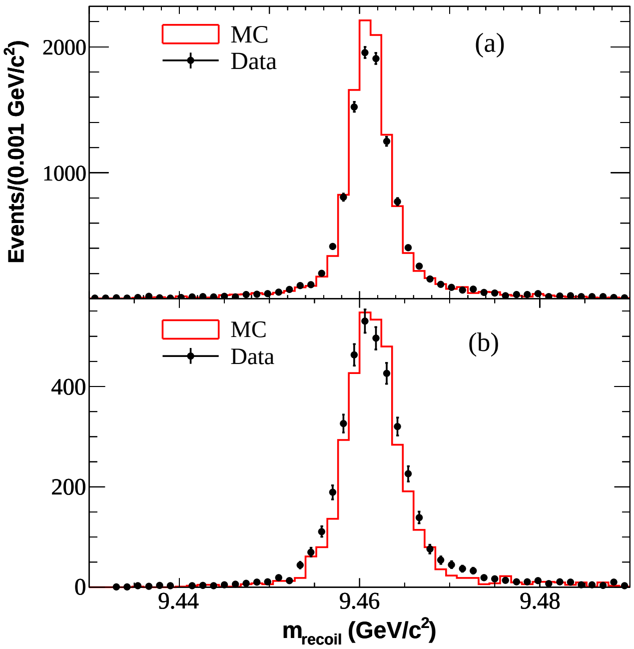

FIG. 1: (color online) The distribution of $m_{\rm recoil}$ for (a) the $\Upsilon(2S)$ and (b) the $\Upsilon(3S)$ datasets, together with the background predictions from the Monte Carlo (MC) samples, which are dominated by the non-resonant di-muon decays. The MC samples are normalized to the data luminosity.

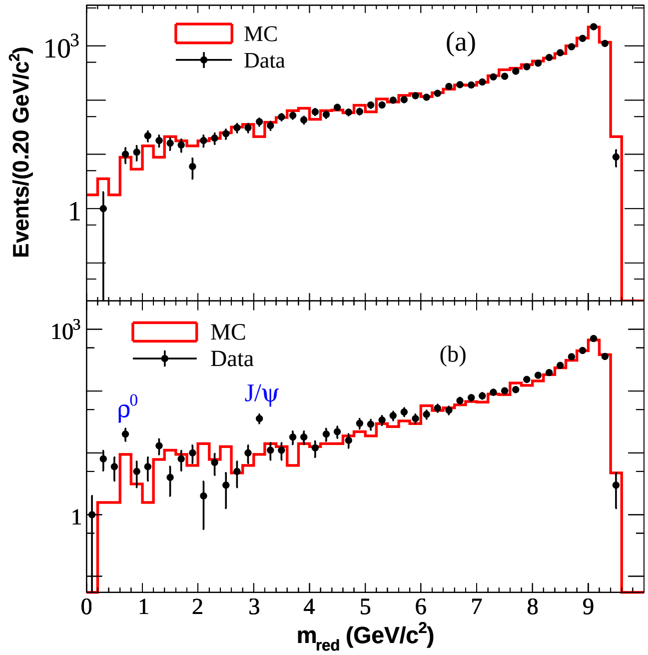

FIG. 2: (color online) The distribution of $m_{\rm red}$ for (a) the $\Upsilon(2S)$ and (b) the $\Upsilon(3S)$ datasets, together with the background predictions from the various Monte Carlo (MC) samples. The MC samples are normalized to the data luminosity. Two peaking components corresponding to the ρ^0 and J/ψ mesons are observed in the $\Upsilon(3S)$ dataset. The contribution of J/ψ mesons is not included in the MC predictions, whereas the ρ^0 meson is poorly modeled in the MC.

old $m_{\mu^+\mu^-} \approx 2m_\mu$ ($m_{\rm red} \approx 0$). After unblinding the data, two peaking components corresponding to ρ^0 and J/ψ mesons are observed in the $\Upsilon(3S)$ dataset. The ρ^0-mesons are mainly produced in initial state radiation (ISR) events, along with two or more pions. This peak disappears if we require both candidates to be identified as muons in the A^0 reconstruction. The J/ψ mesons arise from $e^+e^- \to \gamma_{ISR}\psi(2S)$, $\psi(2S) \to \pi^+\pi^- J/\psi$, $J/\psi \to \mu^+\mu^-$ decays. The J/ψ and ρ^0 events in the $\Upsilon(2S)$ dataset are suppressed since the di-pion mass distribution in these events is above the kinematic edge of the di-pion mass distribution of $\Upsilon(2S)$ decays, but well within the range of values allowed for the $\Upsilon(3S)$ decays.

We extract the signal yield as a function of m_{A^0} in the region $0.212 \le m_{A^0} \le 9.20$ GeV/c^2 by performing a series of one-dimensional unbinned extended maximum likelihood (ML) fits to the $m_{\rm red}$ distribution. We fit over fixed intervals in the low mass region: $0.002 \le m_{\rm red} \le 1.85$ GeV/c^2 for $0.212 \le m_{A^0} \le 1.50$ GeV/c^2, $1.4 \le m_{\rm red} \le 5.6$ GeV/c^2 for $1.50 < m_{A^0} < 5.36$ GeV/c^2 and $5.25 \le m_{\rm red} \le 7.3$ GeV/c^2 for $5.36 \le m_{A^0} \le 7.10$ GeV/c^2. Above this range, we use sliding intervals $\mu - 0.2$ GeV/$c^2 < m_{\rm red} < \mu + 0.15$ GeV/c^2, where μ is the mean of the reduced mass distribution.

The probability density function (PDF) of the signal is described by a sum of two Crystal Ball (CB) functions [25]. The signal PDF is determined as a function of m_{A^0} using signal MC samples generated at 26 different masses, and by interpolating the PDF parameters between each mass point. The resolution of the $m_{\rm red}$ distribution for signal MC increases monotonically with m_{A^0} from 2 to 9 MeV/c^2, while the signal efficiency decreases from 38.3% (40.4%) to 31.7% (31.6%) for $\Upsilon(2S)$ ($\Upsilon(3S)$) transitions. The background for $m_{A^0} \le 1.5$ GeV/c^2 is described by a threshold function

$$f(m_{\rm red}) \propto [{\rm Erf}(s(m_{\rm red} - m_0)) + 1] + \exp(c_0 + c_1 m_{\rm red}) \quad (1)$$

where s is a threshold parameter and m_0 is determined by the kinematic end point of the $m_{\rm red}$ distribution, and c_0 and c_1 are the coefficients of the polynomial function. These parameters are determined from the MC sample of the non-resonant di-muon decays. In the range of $1.5 < m_{A^0} \le 7.1$ GeV/c^2, the background is modeled with a second order Chebyshev polynomial function and with a first order Chebyshev polynomial function for $m_{A^0} > 7.1$ GeV/c^2. We model the ρ^0 background with a Gaussian function, using the sideband data of the di-pion recoil mass distribution from the $\Upsilon(3S)$ sample to determine its mean and width. The background in the J/ψ mass region is modeled by a CB function using a MC sample of $e^+e^- \to \gamma_{ISR}\psi(2S)$, $\psi(2S) \to \pi^+\pi^- J/\psi$, $J/\psi \to \mu^+\mu^-$ decays.

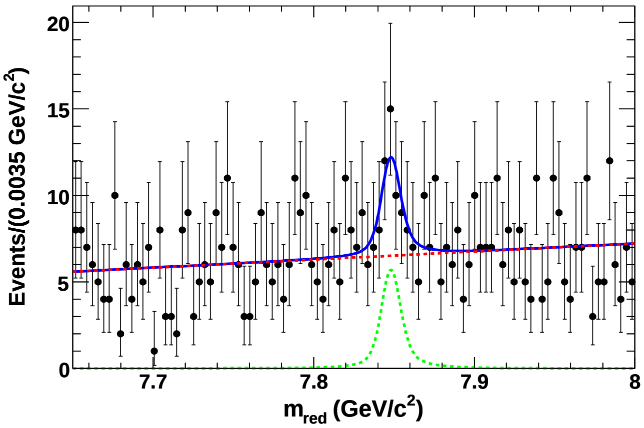

FIG. 3: (color online) Projection plot from the 1d unbinned ML fit to the $m_{\rm red}$ distribution in the $\Upsilon(2S)$ dataset for $m_{A^0} = 7.85\ {\rm GeV}/c^2$ that returns the largest upward fluctuation. The green dotted line shows the contribution of the signal PDF, the magenta dashed line shows the contribution of the continuum background PDF and solid blue line shows the total PDF. The signal peak corresponds to a statistical significance of 3.62σ. Based on the trial factor study, we interpret such observations as mere background fluctuations.

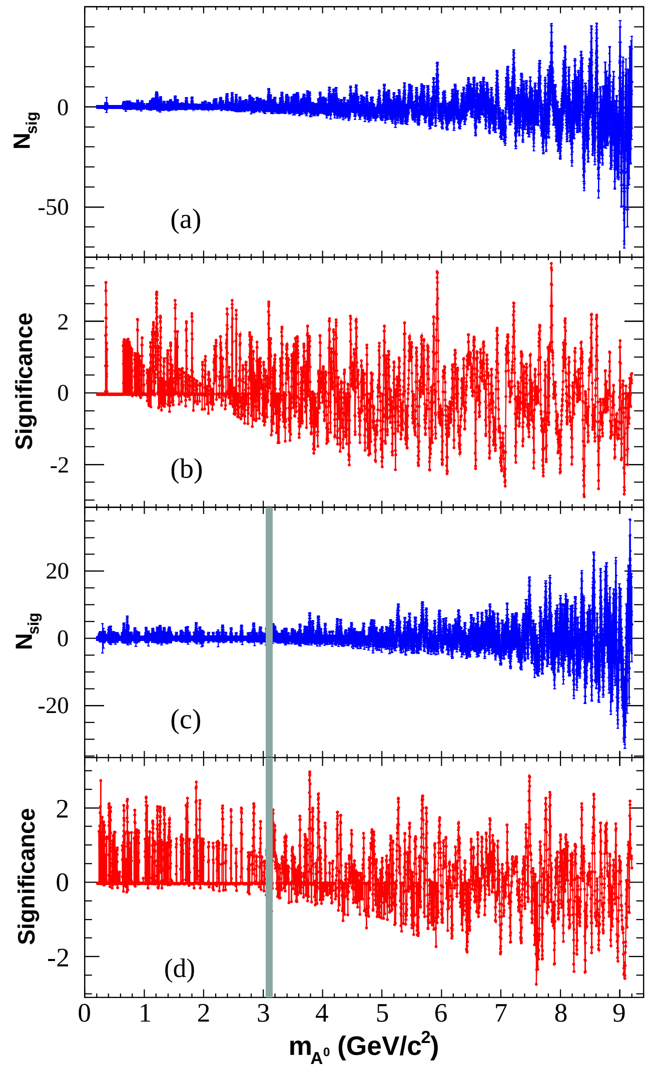

FIG. 4: (color online) The number of signal events (N_{sig}) and significance obtained from the fit as a function of m_{A^0} for (a,b) the $\Upsilon(2S)$ and (c,d) the $\Upsilon(3S)$ datasets. The shaded area shows the region of the J/ψ resonanace, excluded from the search in the $\Upsilon(3S)$ dataset. The impact of the requirement that the total PDF remains non-negative during the ML fit is clearly visible in the lower m_{A^0} region.

We search for the A^0 signal in steps of half the $m_{\rm red}$ resolution, resulting in a total of 4,585 points. The shape of the signal PDF is fixed while the continuum background PDF shape, the signal and background yields are allowed to float. In the fits to the $\Upsilon(3S)$ dataset, we include the ρ^0 background component whose shape is fixed, but we allow its yields to float. The J/ψ mass region in the $\Upsilon(3S)$ dataset, defined as $3.045 \le m_{\rm red} \le 3.162\ {\rm GeV}/c^2$, is excluded from the search due to large background from $J/\psi \to \mu^+\mu^-$ decays. To address the problem associated with the fit involving low statistics, we impose a lower bound on the signal yield by requiring that the total signal plus background PDF remains non-negative [26].

An example of such a fit for $m_{A^0} = 7.85\ {\rm GeV}/c^2$ is shown in Fig. 3. Figure 4 shows the number of signal events (N_{sig}) and the signal significance ($\mathcal{S}$) as a function of m_{A^0}. The signal significance is defined as $\mathcal{S} \equiv {\rm sign}(N_{sig})\sqrt{-2\ln(\mathcal{L}_0/\mathcal{L}_{max})}$, where $\mathcal{L}_{max}$ is the maximum likelihood value for a fit with a floating signal yield centered at m_{A^0}, and $\mathcal{L}_0$ is the likelihood value for $N_{sig} = 0$. The largest values of significance are found to be 3.62σ at $m_{A^0} = 7.85\ {\rm GeV}/c^2$ for $\Upsilon(2S)$ dataset, 2.97σ at $m_{A^0} = 3.78\ {\rm GeV}/c^2$ for $\Upsilon(3S)$ dataset and 3.24σ at $m_{A^0} = 3.88\ {\rm GeV}/c^2$ for the combined $\Upsilon(2S, 3S)$ dataset. We estimate the probability of observing a fluctuation of $\mathcal{S} \ge 3.62\sigma$ ($\mathcal{S} \ge 2.97\sigma$) in the $\Upsilon(2S)$ ($\Upsilon(3S)$) dataset to be 18.1% (66.2%), and for $\mathcal{S} \ge 3.24\sigma$ in the combined $\Upsilon(2S, 3S)$ dataset to be 46.5% based on a large ensemble of pseudo-experiments. Therefore, the distribution of the signal significance is compatible with the null hypothesis.

Tables I and II summarize the additive and multiplicative systematic uncertainties, respectively considered in this analysis. Additive uncertainties arise from the choice of fixed PDF shapes and from a possible bias on the fitted signal yield. The systematic uncertainty associated with the fixed parameters of the PDFs is determined by varying each parameter within its statistical uncertainties while taking correlations between the parameters into account. This uncertainty is found to be small for each mass point and does not scale with the signal yields. We perform a study of a possible fit bias on the signal yield with a large number of pseudo-experiments. The biases are consistent with zero and their average uncertainty is

TABLE I: Additive systematic uncertainties and their sources.

Source	$\Upsilon(2S)$ (events)	$\Upsilon(3S)$ (events)
N_{sig} PDF	(0.00 – 0.62)	(0.04 – 0.58)
Fit Bias	0.22	0.17
Total	(0.22 – 0.66)	(0.17 – 0.60)

TABLE II: Multiplicative systematic uncertainties and their sources.

Source	$\Upsilon(2S)$ (%)	$\Upsilon(3S)$ (%)
Muon-ID	4.30	4.25
Charged tracks	3.73	3.50
$\mathcal{B}(\Upsilon(nS) \to \pi^+\pi^-\Upsilon(1S))$	2.20	2.30
RF classifier	2.21	2.16
Photon efficiency	1.96	1.96
$\Upsilon(nS)$ kinematic fit χ^2	1.52	2.96
$N_{\Upsilon(nS)}$	0.86	0.86
Total	7.00	7.32

taken as a systematic uncertainty.

The multiplicative systematic uncertainties arise from the signal selection and $\Upsilon(nS)$ counting. They include contributions from the RF classifier selection, particle identification, photon selection, tracking and the $\Upsilon(2S, 3S)$ constrained fit. The uncertainty associated with the RF classifier is studied using the non-resonant di-muon decays in both data and MC. We apply the RF selection to these control samples to calculate the relative difference in efficiency between data and MC. The systematic uncertainty related to the photon selection is measured using an $e^+e^- \to \gamma\gamma$ sample in which one of the photon converts into an e^+e^- pair in the detector material [9]. The uncertainties on the branching fractions $\Upsilon(2S, 3S) \to \pi^+\pi^-\Upsilon(1S)$ are 2.2% and 2.3% for the $\Upsilon(2S)$ and $\Upsilon(3S)$ datasets [27], respectively.

We find no significant signal and set 90% confidence level (C.L.) Bayesian upper limits on the product of branching fractions of $\mathcal{B}(\Upsilon(1S) \to \gamma A^0) \times \mathcal{B}(A^0 \to \mu^+\mu^-)$ in the range of $0.212 \le m_{A^0} \le 9.20$ GeV/c^2. Figure 5 shows the branching fraction upper limits at 90% C.L. which are determined with flat priors. The systematic uncertainty is included by convolving the likelihood with a Gaussian distribution having a width equal to the systematic uncertainties described above. The combined result is obtained by simply adding the logarithms of the $\Upsilon(2S, 3S)$ likelihoods. The limits range between $(0.37 - 8.97) \times 10^{-6}$ for the $\Upsilon(2S)$ dataset, $(1.13 - 24.2) \times 10^{-6}$ for the $\Upsilon(3S)$ dataset, and $(0.28 - 9.7) \times 10^{-6}$ for the combined $\Upsilon(2S, 3S)$ dataset.

The branching fractions of $\mathcal{B}(\Upsilon(nS) \to \gamma A^0)$ ($n = 1, 2, 3$) are related to the effective Yukawa coupling (f_Υ) of the b-quark to the A^0 through [5, 28, 29]:

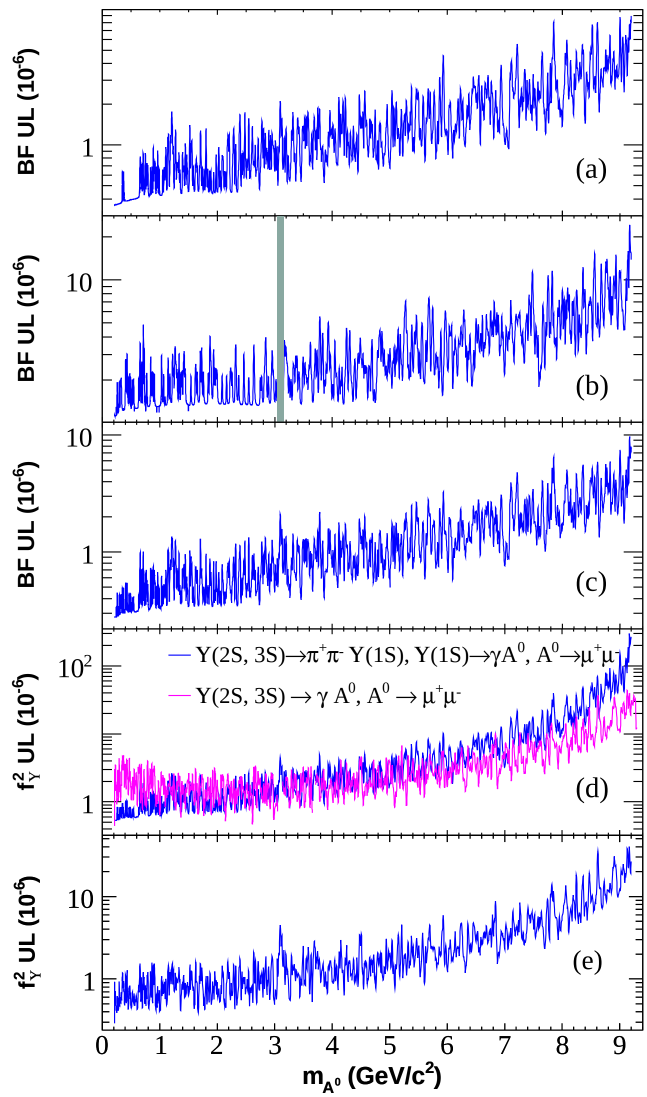

FIG. 5: (color online) The 90% C.L. upper limits (UL) on the product of branching fractions $\mathcal{B}(\Upsilon(1S) \to \gamma A^0) \times \mathcal{B}(A^0 \to \mu^+\mu^-)$ for (a) the $\Upsilon(2S)$ dataset, (b) the $\Upsilon(3S)$ dataset and (c) the combined $\Upsilon(2S, 3S)$ dataset; (d) the 90% C.L. UL on the effective Yukawa coupling $f_\Upsilon^2 \times \mathcal{B}(A^0 \to \mu^+\mu^-)$, together with our previous *BABAR* measurement of $\Upsilon(2S, 3S) \to \gamma A^0$, $A^0 \to \mu^+\mu^-$ [7], and (e) the combined limit. The shaded area shows the region of the J/ψ resonanace, excluded from the search in the $\Upsilon(3S)$ dataset. Details of the UL and Yukawa coupling as a function of m_{A^0} are provided in [32].

$$\frac{\mathcal{B}(\Upsilon(nS) \to \gamma A^0)}{\mathcal{B}(\Upsilon(nS) \to l^+l^-)} = \frac{f_\Upsilon^2}{2\pi\alpha}\left(1 - \frac{m_{A^0}^2}{m_{\Upsilon(nS)}^2}\right), \qquad (2)$$

where $l \equiv e$ or μ and α is the fine structure constant. The value of f_Υ incorporates the QCD and relativistic corrections to $\mathcal{B}(\Upsilon(nS) \to \gamma A^0)$ [29], as well as the leptonic width of $\Upsilon(nS) \to l^+l^-$ [30]. These corrections are as large as 30% to first order in the strong coupling constant

(α_S), but have comparable uncertainties [31]. The 90% C.L. upper limits on $f_{\Upsilon}^2 \times \mathcal{B}(A^0 \to \mu^+\mu^-)$ for combined $\Upsilon(2S, 3S)$ datasets range from 0.54×10^{-6} to 3.0×10^{-4} depending upon the mass of the A^0, which is shown in Fig. 5(d). We combine these results with our previous measurements of $\Upsilon(2S, 3S) \to \gamma A^0$, $A^0 \to \mu^+\mu^-$ [7], to obtain 90% C.L. upper limits on $f_{\Upsilon}^2 \times \mathcal{B}(A^0 \to \mu^+\mu^-)$ in the range of $(0.29 - 40) \times 10^{-6}$ for $m_{A^0} \leq 9.2$ GeV/c^2 (Fig. 5(e)).

In summary, we find no evidence for a light scalar Higgs boson in the radiative decays of $\Upsilon(1S)$ and set 90% C.L. upper limits on the product branching fraction of $\mathcal{B}(\Upsilon(1S) \to \gamma A^0) \times \mathcal{B}(A^0 \to \mu^+\mu^-)$ in the range of $(0.28 - 9.7) \times 10^{-6}$ for $0.212 \leq m_{A^0} \leq 9.20$ GeV/c^2. These results improve the current best limits by a factor of 2–3 for $m_{A^0} < 1.2$ GeV/c^2 and are comparable to the previous *BABAR* results [7] in the mass range of $1.20 < m_{A^0} < 3.6$ GeV/c^2. We also set limits on the product $f_{\Upsilon}^2 \times \mathcal{B}(A^0 \to \mu^+\mu^-)$ at the level of $(0.29 - 40) \times 10^{-6}$ for $m_{A^0} \leq 9.2$ GeV/c^2.

We are grateful for the extraordinary contributions of our PEP-II colleagues in achieving the excellent luminosity and machine conditions that have made this work possible. The success of this project also relies critically on the expertise and dedication of the computing organizations that support *BABAR*. The collaborating institutions wish to thank SLAC for its support and the kind hospitality extended to them. This work is supported by the US Department of Energy and National Science Foundation, the Natural Sciences and Engineering Research Council (Canada), the Commissariat à l'Energie Atomique and Institut National de Physique Nucléaire et de Physique des Particules (France), the Bundesministerium für Bildung und Forschung and Deutsche Forschungsgemeinschaft (Germany), the Istituto Nazionale di Fisica Nucleare (Italy), the Foundation for Fundamental Research on Matter (The Netherlands), the Research Council of Norway, the Ministry of Education and Science of the Russian Federation, Ministerio de Educación y Ciencia (Spain), and the Science and Technology Facilities Council (United Kingdom). Individuals have received support from the Marie-Curie IEF program (European Union) and the A. P. Sloan Foundation.

[1] G. Hiller, Phys. Rev. **D 70**, 034018 (2004); R. Dermisek and J. F. Gunion, Phys. Rev. Lett. **95**, 041801 (2005).
[2] R. Dermisek, J. F. Gunion and B. McElrath, Phys. Rev. **D 76**, 051105 (2007).
[3] H. E. Haber and G. L. Kane, Phys. Rep. **117**, 75 (1985).
[4] J. E. Kim and H. P. Niles, Phys. Lett. **B 138** 150 (1984).
[5] F. Wilczek, Phys. Rev. Lett. **39**, 1304 (1977).
[6] M. Lisanti and J. G. Wacker, Phys. Rev. **D 79**, 115006 (2009).
[7] B. Aubert *et al.* [*BABAR* Collaboration], Phys. Rev. Lett. **103**, 081803 (2009).
[8] B. Aubert *et al.* [*BABAR* Collaboration], Phys. Rev. Lett. **103**, 181801 (2009).
[9] P. del Amo Sanchez *et al.* [*BABAR* Collaboration], Phys. Rev. Lett. **107**, 021804 (2011).
[10] J. P. Lees *et al.* [*BABAR* Collaboration], Phys. Rev. Lett. **107**, 221803 (2011).
[11] W. Love *et al.* [CLEO Collaboration], Phys. Rev. Lett. **101**, 151802 (2008).
[12] M. Ablikim *et al.* [BESIII collaboration], Phys. Rev. **D 85**, 092012 (2012).
[13] S. Chatrchyan *et al.* [CMS collaboration], Phys. Rev. Lett. **109**, 121801 (2012).
[14] R. Dermisek and J.F. Gunion, Phys. Rev. **D 81**, 075003 (2010); F. Domingo, JHEP **1104**, 016 (2011).
[15] E. Fullana and M.A. Sanchis-Lozano, Phys. Lett. **B 653**, 67 (2007).
[16] B. Aubert *et al.* [*BABAR* Collaboration], Nucl. Instrum. Methods Phys. Res., Sect. **A 479**, 1 (2002).
[17] M. Andreotti *et al.* [*BABAR* Collaboration], SLAC-PUB-12205 (2005); F. Anulli et al., Nucl. Instrum. Methods Phys. Res., Sect. **A 515**, 322 (2003).
[18] D. J. Lange, Nucl. Instrum. Meth. A **462**, 152 (2001).
[19] S. Jadach, W. Placzek, B.F.L. Ward, Phys. Lett. **B 390** 298 (1997).
[20] B. F. L. Ward, S. Jadach and Z. Was, Nucl. Phys. Proc. Suppl. **116**, 73 (2003).
[21] D. Cronin-Hennessy *et al.* [CLEO Collaboration], Phys. Rev. **D 76** 072001 (2007).
[22] S. Agostinelli *et al.* [GEANT4 Collaboration], Nucl. Instrum. Methods Phys. Res., Sect. **A 506** 250 (2003).
[23] L. Breiman, Machine Learning **45** 5-32 (2001).
[24] G. Punzi, Sensitivity of searches for new signals and its optimization, arXiv:physics/0308063 (2003).
[25] M. J. Oreglia, Ph.D Thesis, report SLAC-236 (1980); J.E. Gaiser, Ph.D Thesis, report SLAC-255 (1982); T. Skwarnicki, Ph.D Thesis, report DESY F31-86-02 (1986).
[26] B. Aubert *et al.* [*BABAR* Collaboration], Phys. Rev. Lett. **88**, 241801 (2002).
[27] J. Beringer *et al.* [Particle Data Group], Phys. Rev. **D 86**, 010001 (2012).
[28] M. L. Mangano and P. Nason, Mod. Phys. Lett. **A 22**, 1373 (2007).
[29] P. Nason, Phys. Lett. **B 175**, 223 (1986).
[30] R. Barbieri *et al.*, Phys. Lett. **B 57**, 455 (1975).
[31] M. Beneke, A. Signer and V.A. Smirnov, Phys. Rev. Lett. **80**, 2535 (1998).
[32] EPAPS Document No. [XXXXX]. For more information on EPAPS, see http://www.aip.org/pubservs/epaps.html.